P H Y S I C A L   R E V I E W   L E T T E R S

Stabilizing Topological Phases in Graphene via Random Adsorption

Hua Jiang,[1,*] Zhenhua Qiao,[2,†] Haiwen Liu,[3] Junren Shi,[1] and Qian Niu[2,1]

[1]*International Center for Quantum Materials, Peking University, Beijing 100871, China*
[2]*Department of Physics, The University of Texas at Austin, Austin, Texas 78712, USA*
[3]*Institute of Physics, Chinese Academy of Sciences, Beijing 100190, China*
(Received 16 April 2012; published 11 September 2012)

We study the possibility of realizing topological phases in graphene with randomly distributed adsorbates. When graphene is subjected to periodically distributed adatoms, the enhanced spin-orbit couplings can result in various topological phases. However, at certain adatom coverages, the intervalley scattering renders the system a trivial insulator. By employing a finite-size scaling approach and Landauer-Büttiker formula, we show that the randomization of adatom distribution greatly weakens the intervalley scattering, but plays a negligible role in spin-orbit couplings. Consequently, such a randomization turns graphene from a trivial insulator into a topological state.

Introduction.—Due to its unusual structure, graphene displays two other internal degrees of freedom besides the real spin: *AB* sublattice and valleys K/K' [1]. When graphene is deposited on substrates or adsorbed with heavy atoms, the interaction-induced symmetry breaking can open bulk gaps to support kinds of topological phases. For example, a staggered *AB* sublattice potential breaking the inversion symmetry leads to a quantum valley-Hall effect [2–4]; certain nonmagnetic adatoms [5] can enhance the intrinsic spin-orbit coupling (SOC) of graphene to host a quantum spin-Hall state [6]; some $3d$ or $5d$ transition metal adatoms produce a quantum anomalous-Hall state [7–9] due to the interplay between proximity-induced magnetization and Rashba SOC [10]. It is noteworthy that the intervalley scattering in these studies is completely avoided by choosing appropriate adatom coverages with valleys being separated in the momentum space, e.g., one adatom in each 4×4 supercell of graphene.

However, at some specific adatom coverages, i.e., one adatom in each $3n \times 3n$ ($n = 1, 2, 3, ...$) supercell of graphene, valleys K and K' are folded into the Γ point. The resulting intervalley scattering becomes significant and drives graphene into a trivial insulator [10,11]. In realistic samples, the precise control of periodic adsorption is impractical. The randomly distributed adatoms inevitably cause mixture of different coverages and introduce the intervalley scattering. These have discouraged experimentalists from exploring such novel states. Therefore, a crucial issue arises: taking the site randomization of adatoms into account, is it possible to observe topological phases experimentally?

In this Letter, we show that the randomization of adatom distribution greatly weakens the intervalley scattering, but does not affect the induced SOCs and magnetization, suggesting prosperity of realizing topological phases in graphene. Using a finite-size scaling method, we show that the randomization can induce a topological phase transition

from a trivial insulator to a topological insulator. With the Landauer-Büttiker formula, we confirm our finding by computing the two-terminal conductance under periodically or randomly distributed adatoms.

Quantum spin-Hall effect.—We consider a graphene sheet adsorbed with nonmagnetic atoms (e.g., indium or thallium), which prefer hollow sites of graphene [5]. For simplicity, we assume that adatoms only interact with the surrounding six-nearest carbon atoms. Such an interaction enhances the intrinsic SOC and generates a site potential (also known as the crystal field stabilization energy) on each influenced carbon atom. This potential is key to induce the intervalley scattering.

The tight-binding Hamiltonian of graphene with randomly distributed adatoms reads [5,6,12]:

$$H = -t \sum_{\langle ij \rangle, \alpha} c_{i\alpha}^{\dagger} c_{j\alpha} + i\lambda_{\mathrm{SO}} \sum_{\langle\langle ij \rangle\rangle \in \mathcal{R}, \alpha\beta} \nu_{ij} c_{i\alpha}^{\dagger} s_{\alpha\beta}^{z} c_{j\beta}$$
$$+ U \sum_{i \in \mathcal{R}, \alpha} c_{i\alpha}^{\dagger} c_{i\alpha}, \qquad (1)$$

where $c_{i\alpha}^{\dagger}$ creates an electron on site i with spin α, and t is the hopping energy between nearest neighbors. The last two terms represent respectively the intrinsic SOC λ_{SO} and site potential U, which apply on the influenced sites denoted by $\mathcal{R}$. s_z is the z-component of spin Pauli matrices. $\langle\langle ... \rangle\rangle$ sums over all next-nearest neighbors. $\nu_{ij} = 1(-1)$ corresponds to the hopping clockwise (counterclockwise) between next-nearest neighbors. According to their formation mechanisms, λ_{SO} should be one order smaller than U. In the following, we adopt the intrinsic SOC in the thallium-atom adsorption case, i.e., $\lambda_{\mathrm{SO}} = 0.016t \approx 0.044$ eV [5].

As mentioned in the Introduction, topological phases in graphene are sensitive to the coverage of adatoms. To make our investigation complete and convincing, we shall discuss the effect of randomization on two kinds of adatom coverage with and without intervalley scattering. We begin

with the discussion on the 11.1% adatom coverage with intervalley scattering.

Let us first examine the sensitivity of topologically trivial or nontrivial phases to the adatom configuration. Figures 1(a) and 1(b) display two different 6×6 supercells of graphene. To keep the coverage, four adatoms are included in each supercell. In Fig. 1(a), the 3×3 periodicity still holds, while in Fig. 1(b) the 3×3 translational symmetry is broken due to the shift of one adatom to its neighboring site. This can be regarded as the simplest step to randomize a 3×3 supercell to a 6×6 one. To understand the role of randomization on the site potential U and intrinsic SOC λ_{SO}, we plot the bulk band structure around the Γ point by considering only U or λ_{SO}. In the presence of only U, the intervalley scattering in the 3×3 supercell opens a bulk gap as plotted in the solid line in Fig. 1(c). Due to the spin and valley degeneracy, the bulk bands are fourfold degenerate. One can see that a slight change of the adatom configuration lifts the valley degeneracy (see dashed bands) and shrinks the bulk band gap, implying the decrease of the intervalley scattering. As a sharp contrast, the band structures with only intrinsic SOC are almost identical for both supercells [see Fig. 1(d)]. This indicates that the effect of intrinsic SOC is insensitive to the slight change of the adatom configuration.

Although both site potential and intrinsic SOC can open bulk gaps, the resulting insulators are topologically different.
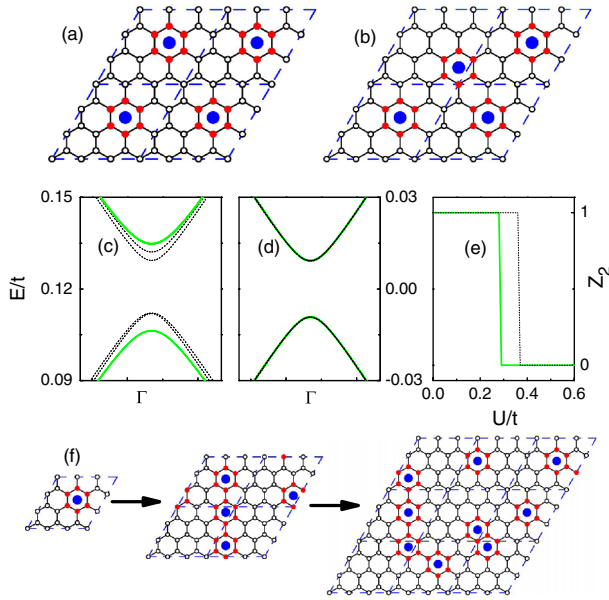

FIG. 1 (color online). (a)–(b) Two different configurations of 4 adatoms in a 6×6 supercell. (c)–(d) Bulk band structure only with site potential $U = 0.36t$ (c) or intrinsic SOC $\lambda_{SO} = 0.016t$ (d). (e) Z_2 topological number versus U at fixed $\lambda_{SO} = 0.016t$. In (c)-(e), solid and dashed lines correspond respectively to the supercells in (a) and (b). (f) Schematic of the finite-size scaling at a fixed 11.1% adatom coverage. Empty, small solid and large solid circles represent the pristine graphene, carbons influenced by adatoms, and adatoms, respectively.

An efficient way to identify these phases is to calculate the Z_2 topological number. Using the methods discussed in Refs. [13,14], we find different phases arising from the competition between U and λ_{SO}. As shown in Fig. 1(e), for a fixed $\lambda_{SO} = 0.016t$, small U leads to a $Z_2 = 1$ quantum spin-Hall insulator, while large U gives rise to a $Z_2 = 0$ trivial insulator. A remarkable difference between the two configurations can be observed in the range of $U \in [0.29t, 0.36t]$: a phase transition occurs from a trivial insulator to a $Z_2 = 1$ topological insulator.

Through employing a finite-size scaling method, we study the effect of strong randomization of adsorption sites. The simulation procedures can be summarized as follows: (1) expanding the supercell from 3×3 to $3n \times 3n$ ($n = 2, 3, 4...$); (2) randomly selecting n^2 hollow sites and then determining the influenced atomic sites $\mathcal{R}$; (3) based on the Hamiltonian in Eq. (1), calculating the bulk band structure and measuring the bulk gap Δ; (4) repeating the steps (2) and (3) to obtain M samples. Thereupon, the probability distribution of bulk gap $P(\Delta)$ can be obtained according to $P(\Delta)\delta\Delta = m/M$, where m counts the magnitudes located within the range of $[\Delta - \delta\Delta/2, \Delta + \delta\Delta/2]$.

Figure 2 exhibits the evolution of the probability distribution of bulk gap $P(\Delta)$ along with the increasing of the supercell size n. The left column corresponds to the case with only the site potential $U = 0.36t$. For $n = 1$, although there are 9 different adatom configurations, their band structures are exactly the same. Therefore, the resulting bulk gap is a constant $\Delta = 0.029t$ [see Fig. 2(a)]. When $n > 1$, there are $C_{9n^2}^{n^2}$ adatom configurations in a $3n \times 3n$ supercell, most of which result in distinct band structures. In Figs. 2(d) and 2(e), we observe that the band gap Δ fluctuates in a wide region, and the gap region shrinks toward zero for larger n. To better reflect this characteristic, we introduce the median of each ensemble $\bar{\Delta}$, which is highlighted in a solid red line. After a numerical fitting, a scaling law is found to be $\bar{\Delta} \approx 0.22U^2/(nt)$. Moreover, such power law decay as a function of n can also be analytically obtained from the Fourier component of randomly distributed site potentials corresponding to the intervalley scattering. In the inset of Fig. 2(e), we show that $P(\Delta)$ of $n = 9$ can be fitted by a 2D Maxwell distribution function $f(\Delta) = \Delta/\sigma^2 \exp(-\Delta^2/2\sigma^2)$, where $\sigma = \bar{\Delta}/\sqrt{2\ln 2}$. According to $f(\Delta)$, the probability of opening a band gap in the range of $[3\bar{\Delta}, \infty)$ is about 0.2%. Together with the fact that a realistic sample resembles a $n \rightarrow \infty$ supercell, one can conclude that the intervalley scattering should be vanishing with randomly distributed adsorbates.

Next, we turn to the case with only the intrinsic SOC $\lambda_{SO} = 0.016t$. As shown in the middle column, we find that the bulk gap $\Delta \approx 1.15\lambda_{so}$ is almost independent of the randomization for any supercell size n. This means that the intrinsic SOC remains insensitive to the strong randomization of adatom distribution, and the resulting quantum spin-Hall phase is stable against the random adsorption.
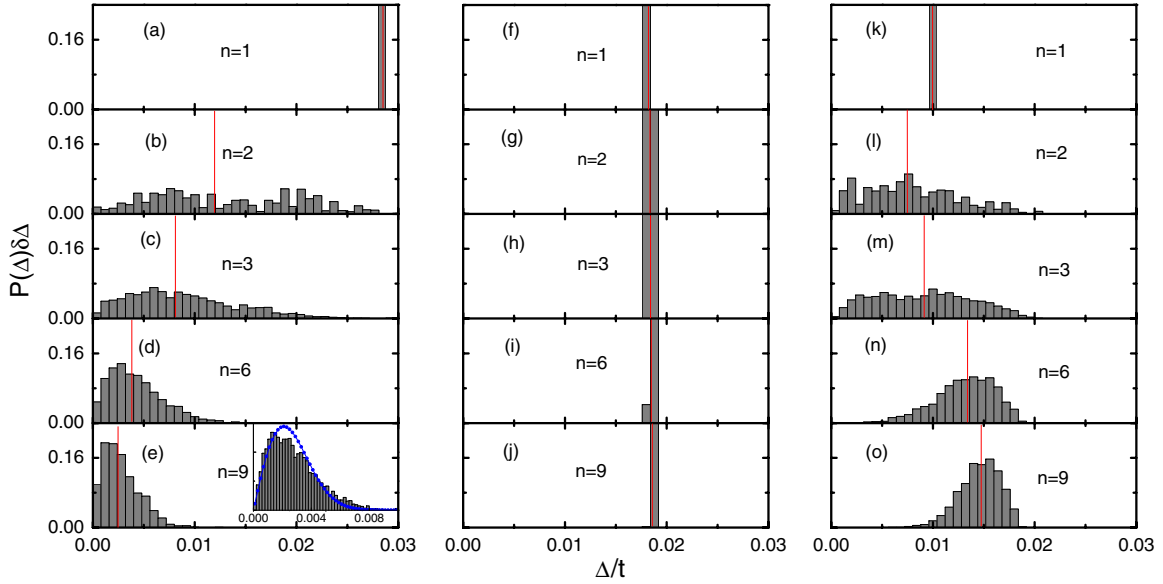
FIG. 2 (color online). Probability distribution of bulk gap $P(\Delta)$ for $3n \times 3n$ supercells of graphene subjected to n^2 randomly distributed adatoms. 2000 samples are collected for each panel. (a)–(e) Only the site potential $U = 0.36t$ is considered. (f)–(j) Only the intrinsic SOC $\lambda_{SO} = 0.016t$ is considered. (k)–(o) Both $U = 0.36t$ and $\lambda_{SO} = 0.016t$ are included. The solid red line labels the median of each ensemble $\bar{\Delta}$. Inset: Numerical fitting of the probability distribution for $n = 9$.

Comparing the results from both limits of only site potential or intrinsic SOC, it is natural to expect that the realistic graphene sample should favor the quantum spin-Hall state when both U and λ_{SO} are present.

Such a speculation is verified by the gap statistics drawn in the right column. In the 3×3 supercell, because of the competition between U and λ_{SO}, the gap opening is smaller than those shown in Figs. 2(a) and 2(f). When the supercell size increases, the median $\bar{\Delta}$ first decreases at $n = 2$, but then increases for larger n [see Figs. 2(m)–2(o)]. The topological number $Z_2 = 0$ is obtained for $n = 1$, whereas $Z_2 = 1$ is found for $n = 3, 6$, and 9. It is thus evident that the increasing of randomization turns graphene from a trivial insulator to a quantum spin-Hall insulator. From the tendency of $\bar{\Delta}$, one can notice that it gradually approaches the band gap labeled in Fig. 2(f).

Thus far, we analyze the influence of randomization by investigating the bulk band structures of various supercells. Below, we design a two-terminal device illustrated in Figs. 3(a) and 3(b) to study the transport properties using the Landauer-Büttiker formula [15]. The adatoms are only considered in the central scattering regime, and two leads are modeled by pristine graphene ribbons. The presence of helical edge modes in the quantum spin-Hall insulator gives rise to a quantized longitudinal conductance.

Figure 3(c) plots the average conductance G and its fluctuation δG as a function of the Fermi energy ε_F. The parameters are $U = 0.36t$ and $\lambda_{SO} = 0.016t$. In the presence of periodically distributed adatoms [see Fig. 3(a)], $G = 0$ and $\delta G = 0$ in units of e^2/h within the range of $\varepsilon_F \in [0.117t, 0.124t]$, signaling a trivial insulator. However,

when the adatoms become randomly distributed in Fig. 3(b), a quantized plateau $G = 2e^2/h$ with vanishing fluctuation emerges in the regime of $\varepsilon_F \in [0.116t, 0.132t]$. The distribution of local currents illustrated in the inset of (c) further indicates a quantum spin-Hall insulator. Such a phase transition resembles the disorder-induced topological Anderson insulator [16,17], except that it is the adatom configuration that triggers the phase transition rather than the disorder strength.

Previous analysis has focused on the 11.1% adatom coverage with strong intervalley scattering. What happens for other coverages without intervalley scattering? Let us consider a 6.25% adatom coverage (one adatom in a 4×4 supercell for example). Using the same finite-size scaling method, we show that the bulk gap is only dependent on the intrinsic SOC, but independent of the site energy or supercell size. An immediate evidence is the robust quantized plateau shown in Fig. 3(d) for either periodically or randomly distributed adatoms. To conclude, in a thallium-atom adsorbed graphene, the quantum spin-Hall state is a system-preferred ground state for any adatom coverage, and the bulk gap ~ 46 meV can be detected under current experimental techniques.

In realistic samples, some adatoms are inevitably distributed on top sites. A staggered sublattice potential can open a trivial gap due to the inversion symmetry breaking. Since adatoms are equally adsorbed on top of A/B sublattices, we show that the randomization of distribution eliminates the effective staggered potential and decrease the trivial gap [18]. Therefore, the top adsorption does not affect the realization of topological states in graphene.
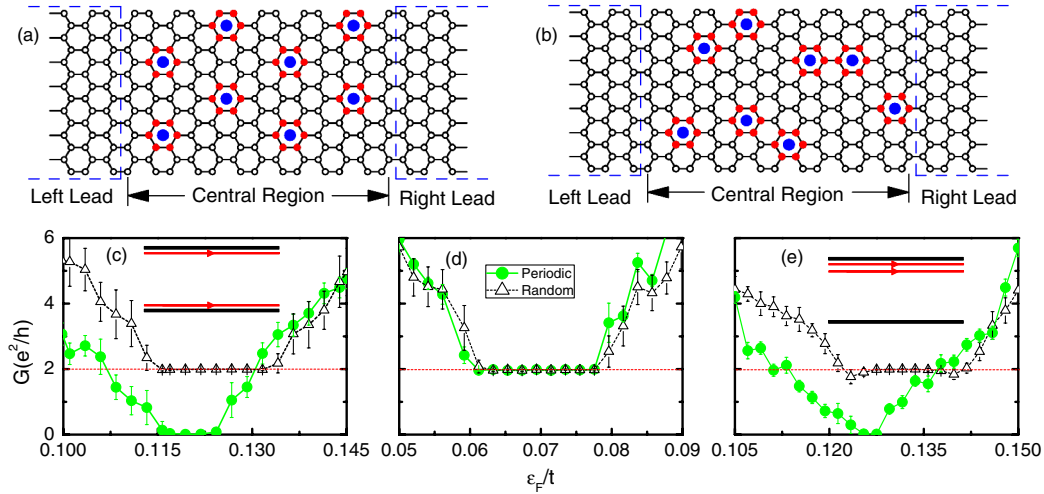
FIG. 3 (color online).   (a)–(b) Schematic of a two-terminal setup with periodically and randomly distributed adatoms, respectively. Both adatom coverages are 11.1%. (c)–(e) Comparison of conductances G between periodic and random adsorption as a function of Fermi level ε_F. (c)–(d) The site potential and intrinsic SOC are set to be $U = 0.36t$ and $\lambda_{SO} = 0.016t$. The adatom coverages are 11.1% in panel (c) and 6.25% in panel (d). In (e), the site potential, Rashba SOC, and magetization are set to be $U = 0.38t$, $\lambda_R = 0.04t$, and $M = 0.04t$, respectively. The adatom coverage is 11.1%. Circle and triangle symbols represent the periodic and random adatoms. The associated error bar denotes the conductance fluctuation δG. Insets of (c) and (e): schematic of the quantized channels from left to right.

In semiconductors with weak disorder, the spin-Hall conductance vanishes for uniform SOC [19], whereas a finite but non-universal spin-Hall conductance emerges for spatially random SOC [20]. In contrast, when the system exhibiting a quantum spin-Hall effect is subjected to uniform or random SOC, as long as the Fermi level lies inside the bulk gap, the spin-Hall conductance is universally quantized and topologically protected against weak disorders.

Quantum anomalous-Hall effect.—When the $3d/5d$ transition metal atoms are adsorbed on graphene, the interaction enhances Rashba SOC λ_R [21], and induces site potential U and magnetization M. In Refs. [8–10], *ab initio* calculations show that the quantum anomalous-Hall phase can be produced in the 6.25% adatom coverage, but the trivial insulator is usually formed in the 11.1% adatom coverage due to the strong intervalley scattering. In Fig. 3(e), we calculate the average conductance versus the Fermi energy ε_F at 11.1% adatom coverage. The parameters are $U = 0.38t$, $\lambda_R = 0.04t$, and $M = 0.04t$. We observe that $G = 0e^2/h$ in the range of $\varepsilon_F \in [0.125t, 0.127t]$ for the periodically distributed adatoms. However, for the randomly distributed adatoms, a quantized plateau $G = 2e^2/h$ appears in the range of $\varepsilon_F \in [0.127t, 0.137t]$. The inset plots the schematic of the corresponding local current, indicating a quantum anomalous-Hall insulator. This result further confirms our finding that while the intervalley scattering is fragile, the SOC and exchange field are robust against the randomization of adatom distribution.

Summary.—For periodically distributed adatoms with certain coverage, the strong intervalley scattering plays a dominant role and suppress the topological gap, thus turning

graphene into a trivial insulator. Using both finite-size scaling method and transport calculation, we show that when the adatom distribution becomes random, the intervalley scattering is weakened, but other quantities (e.g., SOCs and magnetization) are not affected. This finding points out that the topological states are graphene-favored ground states in the presence of randomly distributed adatoms.

*jianghuaphy@gmail.com
†zhqiao@physics.utexas.edu
[1] A. H. Castro Neto, F. Guinea, N. M. R. Peres, K. S. Novoselov, and A. K. Geim, Rev. Mod. Phys. **81,** 109 (2009).
[2] S. Y. Zhou, G.-H. Gweon, A. V. Fedorov, P. N. First, W. A. de Heer, D.-H. Lee, F. Guinea, A. H. C. Neto, A. Lanzara, Nature Mater. **6,** 770 (2007).
[3] G. Giovannetti, P. A. Khomyakov, G. Brocks, P. J. Kelly, and J. van den Brink, Phys. Rev. B **76,** 073103 (2007).
[4] D. Xiao, W. Yao, and Q. Niu, Phys. Rev. Lett. **99,** 236809 (2007).
[5] C. Weeks, J. Hu, J. Alicea, M. Franz, and R. Wu, Phys. Rev. X **1,** 021001 (2011); J. Hu, J. Alicea, R. Q. Wu, and M. Franz, arXiv:1206.4320.

[6] C. L. Kane and E. J. Mele, Phys. Rev. Lett. **95,** 146802 (2005); **95,** 226801 (2005).

[7] F. D. M. Haldane, Phys. Rev. Lett. **61,** 2015 (1988).

[8] H. Zhang, C. Lazo, S. Blügel, S. Heinze, and Y. Mokrousov, Phys. Rev. Lett. **108,** 056802 (2012).

[9] J. Ding, Z. H. Qiao, W. X. Feng, Y. G. Yao, and Q. Niu, Phys. Rev. B **84,** 195444 (2011).

[10] Z. H. Qiao, S. A. Yang, W. Feng, W-K. Tse, J. Ding, Y. Yao, J. Wang, and Q. Niu, Phys. Rev. B **82,** 161414(R) (2010); W. K. Tse, Z. Qiao, Y. G. Yao, A. H. MacDonald, and Q. Niu, Phys. Rev. B **83,** 155447 (2011); Z. H. Qiao, H. Jiang, X. Li, Y. G. Yao, and Q. Niu, Phys. Rev. B **85,** 115439 (2012).

[11] A. H. Zhang, H. F. Teoh, Z. Dai, Y. P. Feng, and C. Zhang, Appl. Phys. Lett. **98,** 023105 (2011).

[12] O. Shevtsov, P. Carmier, C. Groth, X. Waintal, and D. Carpentier, Phys. Rev. B **85,** 245441 (2012).

[13] L. Fu and C. L. Kane, Phys. Rev. B **74,** 195312 (2006).

[14] T. Fukui and Y. Hatsugai, J. Phys. Soc. Jpn. **76,** 053702 (2007); A. M. Essin and J. E. Moore, Phys. Rev. B **76,** 165307 (2007);

[15] S. Datta, *Electronic Transport in Mesoscopic systems* (Cambridge University Press, Cambridge, England, 1995).

[16] J. Li, R. L. Chu, J. K. Jain, and S. Q. Shen, Phys. Rev. Lett. **102,** 136806 (2009); H. Jiang, L. Wang, Q.-F. Sun, and X. C. Xie, Phys. Rev. B **80,** 165316 (2009); E. Prodan, Phys. Rev. B **83,** 195119 (2011).

[17] C. W. Groth, M. Wimmer, A. R. Akhmerov, J. Tworzydło, and C. W. J. Beenakker, Phys. Rev. Lett. **103,** 196805 (2009).

[18] See Supplemental Material at http://link.aps.org/supplemental/10.1103/PhysRevLett.109.116803 for details on the model, parameters, numerical methods and results.

[19] E. G. Mishchenko, A. V. Shytov, and B. I. Halperin, Phys. Rev. Lett. **93,** 226602 (2004); J. I. Inoue, G. E. W. Bauer, and L. W. Molenkamp, Phys. Rev. B **70,** 041303 (2004); O. V. Dimitrova, Phys. Rev. B **71,** 245327 (2005).

[20] V. K. Dugaev, M. Inglot, E. Ya. Sherman, and J. Barnaś, Phys. Rev. B **82,** 121310(R) (2010).

[21] The expression of Rashba SOC is given in Ref. [6].